GeoMVD: Geometry-Enhanced Multi-View Generation Model Based on Geometric Information Extraction

Jiaqi Wu 1,2* , Yaosen Chen 1,2† , Shuyuan Zhu 1† University of Electronic Science and Technology of China, Chengdu, China 2 Sobey Media Intelligence Laboratory, Chengdu, China

wjq4dpm@std.uestc.edu.cn, chenyaosen@sobey.com, eezsy@uestc.edu.cn

Abstract

Multi-view image generation holds significant application value in computer vision, particularly in domains like 3D reconstruction, virtual reality, and augmented reality. Most existing methods, which rely on extending single images, face notable computational challenges in maintaining cross-view consistency and generating high-resolution outputs. To address these issues, we propose the Geometryguided Multi-View Diffusion Model, which incorporates mechanisms for extracting multi-view geometric information and adjusting the intensity of geometric features to generate images that are both consistent across views and rich in detail. Specifically, we design a multi-view geometry information extraction module that leverages depth maps, normal maps, and foreground segmentation masks to construct a shared geometric structure, ensuring shape and structural consistency across different views. To enhance consistency and detail restoration during generation, we develop a decoupled geometry-enhanced attention mechanism that strengthens feature focus on key geometric details, thereby improving overall image quality and detail preservation. Furthermore, we apply an adaptive learning strategy that fine-tunes the model to better capture spatial relationships and visual coherence between the generated views, ensuring realistic results. Our model also incorporates an iterative refinement process that progressively improves the output quality through multiple stages of image generation. Finally, a dynamic geometry information intensity adjustment mechanism is proposed to adaptively regulate the influence of geometric data, optimizing overall quality while ensuring the naturalness of generated images. More details can be found on the project page: https://sobeymil.github.io/GeoMVD.com/.

1. Introduction

Multi-view image generation is a fundamental task in the field of computer vision, playing a crucial role in various applications such as 3D modeling, virtual reality, augmented reality, robot perception, and simulation. With the rapid development of "text-to-image" diffusion models, significant progress has been made in single-view image generation [1, 2, 10, 27, 29, 33–35]. These models are capable of generating clear, detail-rich images from textual descriptions, greatly expanding the boundaries of automated content creation. However, extending this technology to multi-view image generation and integrating text, images, and 3D data within a unified framework still faces numerous challenges. Multi-view image generation holds great promise in providing strong technical support for 3D reconstruction, virtual reality, and autonomous driving. However, ensuring crossview consistency, geometric accuracy, and overcoming the computational challenges posed by high-resolution images and large-scale 3D datasets remain critical issues in current research.

Existing multi-view diffusion models generally achieve image generation tasks by fine-tuning "text-to-image" models [7, 12, 17, 20, 21, 25, 26, 37, 38, 40, 42, 46]. These methods model 3D consistency between images by applying attention across multiple views. However, as the resolution of images and the scale of 3D data increase, the computational cost becomes significantly higher. In particular, as model sizes grow and resolution requirements escalate, training and inference processes become computationally expensive, making it difficult to achieve the desired image quality. Moreover, despite some advanced methods being trained on large-scale datasets, the lack of high-quality 3D training data increases the difficulty of optimization, leading to gaps in the generated multi-view image quality in both detail and consistency. Therefore, maintaining image consistency, geometric accuracy, and detail richness while handling large-scale data is a critical issue in current multi-view image generation research.

[†]Corresponding Authors.

^{*}Work done during an internship at SobeyMIL.

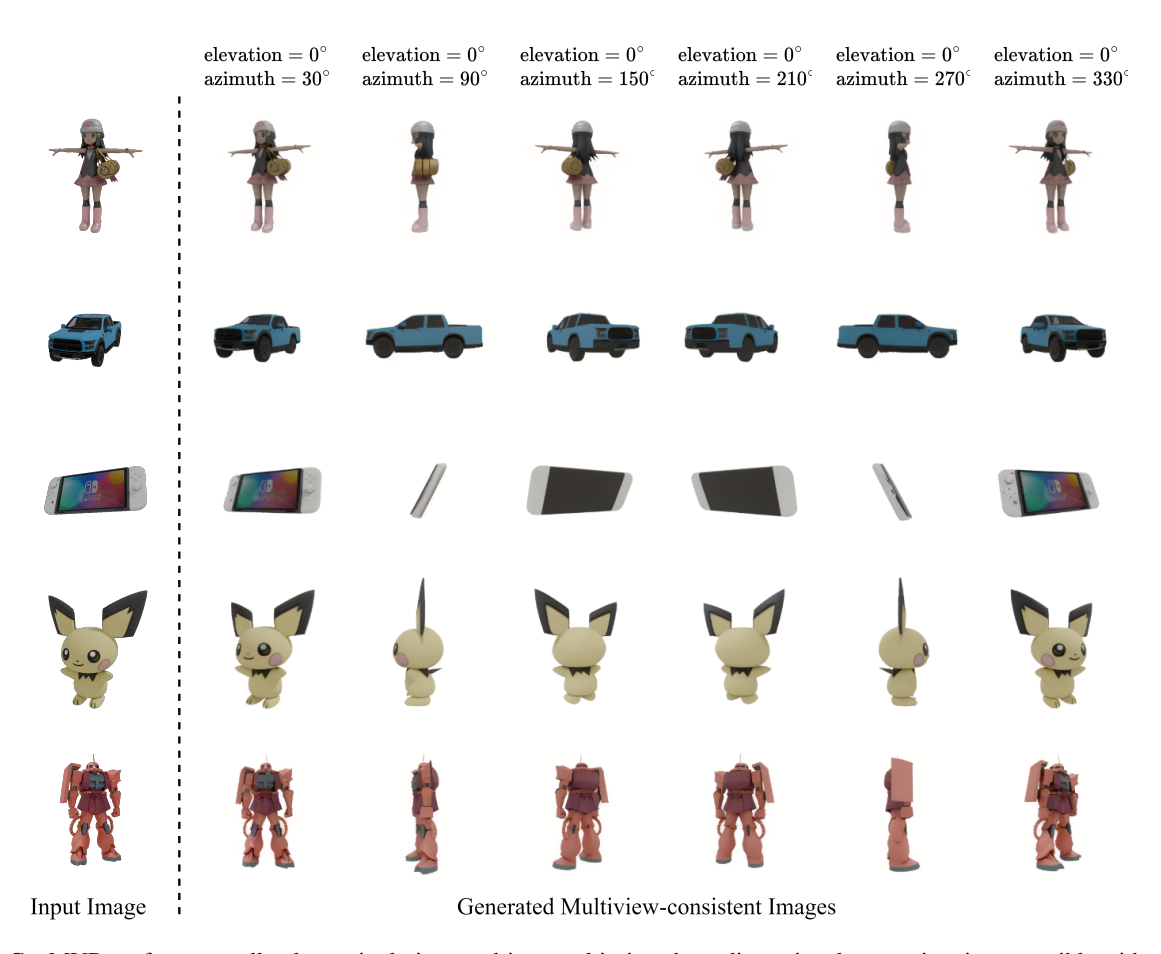


Figure 1. GeoMVD performs excellently on single-image-driven multi-view three-dimensional generation, is compatible with real photographs, synthesized images, and two-dimensional illustrations, and maintains cross-view consistency and high quality.

To address these bottlenecks, we propose a geometryguided multi-view diffusion model. The core idea is to first estimate depth and normal maps from a single input image and combine them with foreground segmentation to construct a continuous, edge-preserving proxy surface via bilateral normal integration. Then, we render the multiview geometry images from the target viewpoints based on this proxy surface, aligning them naturally within a shared geometric framework, thus preventing boundary misalignment, occlusion inconsistencies, and detail drift. The overall pipeline uses "input image, optional text, and multi-view geometry images" as conditions to extract appearance details, cross-modal semantics, and geometric structures, which are jointly utilized at each diffusion step to ensure semantic consistency, geometric accuracy, and appearance fidelity in the generated images.

In terms of feature fusion, we propose a decoupled geometry-enhanced attention mechanism: in addition to selfattention, a parallel geometry attention branch is constructed, with denoising features as the query. The image and geometry conditions are used separately to calculate attention, and then adaptively fused with learnable weights. This significantly strengthens the shape and occlusion constraints across views without sacrificing texture restoration. Considering that geometry is estimated from a single image and may contain errors, we introduce two robustness mechanisms: first, a geometry feature mask based on the cosine similarity between the target viewpoint and the input viewpoint, which adaptively reduces the constraint strength in unreliable views; and second, dynamic adjustment of geometry attention weights according to diffusion steps. Early steps have stronger weights to correct noisy outputs, while later steps reduce the weights to avoid excessive constraints that may damage details. During training, we only add lowrank adaptive fine-tuning parameters to the attention layers, achieving high-resolution generation with minimal trainable parameters and enhanced efficiency and stability.

In summary, our contributions are as follows:

1. We propose a geometry-guided multi-view diffusion framework and multi-view geometry information extrac-

tion module: Depth and normal maps are estimated from a single image and combined with segmentation to construct a proxy surface, which is rendered into multi-view geometry images, providing a shared geometric constraint that systematically enhances cross-view consistency and detail stability.

- We design a triple-condition collaborative denoising process for cross-modal semantics, geometric structure, and image appearance: These three conditions are jointly constrained via cross-attention and subsequent modules, ensuring semantic consistency, structural coherence, and appearance fidelity at each diffusion step.
- 3. We propose a decoupled geometry-enhanced attention mechanism: This mechanism employs a parallel dual-branch attention structure, with one branch processing image features and the other handling geometric features. The final output is obtained by weighted fusion of the attention results from both branches, ensuring consistency and detail preservation across multiple views without over-relying on either geometry or image details.
- 4. We introduce a robust inference strategy: This strategy uses a geometry feature mask based on viewpoint differences and dynamically adjusts geometry attention weights according to diffusion steps. This improves stability and naturalness, ensuring high-quality multi-view generation with minimal computational cost.

2. Related Work

Text-to-Image Diffusion Models. Text-to-image generation has made continuous breakthroughs in the evolution of diffusion models, advancing from basic alignment and efficiency optimization to high resolution, strong controllability, and cross-scene adaptability [1, 4, 8, 10, 14, 15, 29, 33, 34, 39, 45]. Guided diffusion [8] and classifier-free guidance[14] established the foundation for text-conditioned image generation; DALL-E 2 [33] leveraged CLIP [31] to achieve precise text-image alignment; latent diffusion models[34] enhanced efficiency through latent space diffusion; and Stable Diffusion XL [29] optimized high-frequency details with a two-stage cascaded architecture. Recent developments have introduced the Flow Matching[23] technique as an efficient alternative framework, enabling smooth noiseto-image transformation through continuous dynamic flow mapping, significantly reducing sampling steps and improving generation stability. Stable Diffusion 3(SD3)[10] and FLUX are both based on the Diffusion Transformer[28] architecture and utilize flow matching techniques to improve text-image alignment accuracy. SD3 integrates two CLIP encoders and one T5[32] encoder, optimizing text condition processing and image detail generation, thereby enhancing prompt adherence and image generation precision. In contrast, FLUX[1] enhances image style consistency, multiround editing task responsiveness, and multimodal context

processing through its "Kontext" model series, significantly improving the stability and editability of high-resolution generation.

Multiview Generation Based on T2I Models. Multiview generation methods [7, 12, 17, 20, 21, 25, 26, 38, 40, 46] have expanded text-to-image models by leveraging largescale 3D datasets [6, 22, 43] For example, MVDream [38] integrates camera embedding and extends self-attention from 2D to 3D to enable cross-view coherence; SPAD [20] enhances cross-view attention by applying epipolar constraints. Zero123 [24] presents a conditional diffusion method to generate consistent multiviews from a single view, improving cross-view coherence though still limited under high resolution and complex scenes; Zero123++ [37] refines this by introducing more efficient feature extraction strategies to enhance precision and style consistency in multiview generation. Era3D [21] introduces an epipolar-aligned row-level self-attention mechanism, improving stability in multiview generation; SyncDreamer [25] proposes a synchronized multiview diffusion model that leverages 3D-aware attention for improved geometric consistency and image quality. NVS-Adapter [19] introduced a plug-and-play module for pretrained T2I models, specifically for novel view synthesis from a single image. It uses view-consistency cross-attention to align local features across views and global semantic conditioning to align the semantic structure of generated views with a reference view, achieving geometrically consistent multiview synthesis without full model fine-tuning. Building on this, MV-Adapter [18] further extends the concept, offering a plug-and-play adapter that enables pretrained T2I models to perform multiview generation efficiently by preserving their feature space and structure. MV-Adapter significantly enhances the generation performance and application diversity by ensuring better compatibility with various multiview tasks.

Despite these advances, many methods still require large-scale parameter updates to pretrained T2I models, limiting compatibility with model derivatives. This study introduces GeoMVD, a geometry-guided multiview diffusion model. GeoMVD introduces a multiview geometry extraction module, a triplet-condition collaborative denoising process, a decoupled geometry-enhanced attention mechanism, and a geometry-information intensity adjustment mechanism. These innovations significantly improve image quality, consistency, and detail fidelity, outperforming existing methods in cross-view consistency, geometric precision, and generation quality.

3. Method

The overall process of the multi-view diffusion model proposed in this study is illustrated in Fig.2. The input to the

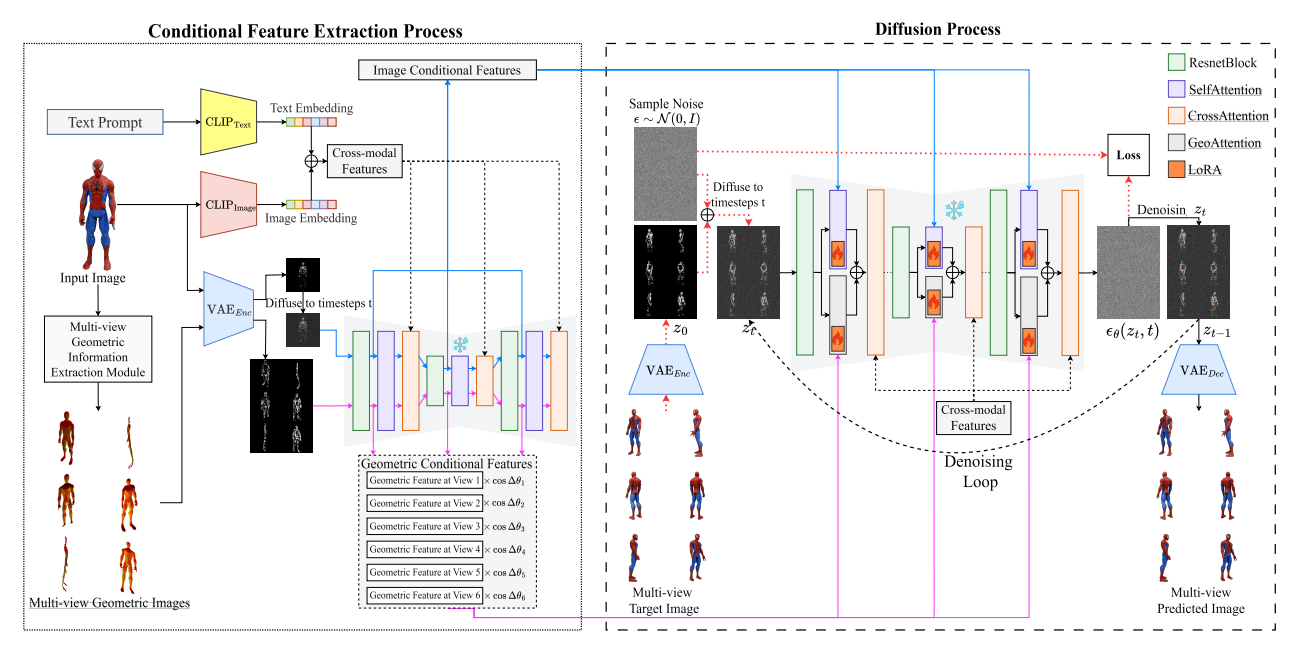


Figure 2. The process of the multi-view diffusion model guided by geometric information.

diffusion model consists of: an image containing the target object, an optional textual description, and multi-view geometric images. These geometric images are generated from the multi-view geometric information extraction module (Section 3.1), which predicts geometric features from a single image under multiple views. During the conditional feature extraction process (Section 3.2), these three inputs are transformed into cross-modal, multi-view geometric, and image conditional features using pre-trained models such as VAE, CLIP, and DiffusionUnet. The cross-modal conditional features are input to the cross-attention layer of the U-Net, while image and multi-view geometric features are processed by the decoupled geometry-enhanced attention module (Section 3.3). Additionally, the geometric information intensity modulation mechanism (Section 3.4) dynamically adjusts the strength of the geometric guidance during the generation process to ensure stable and effective constraints.

3.1. Multi-view Geometric Information Extraction Module

Traditional multi-view diffusion models generate multi-view images directly from a single image. However, due to the absence of reliable 3D geometric priors, these models often struggle with structural consistency across views, leading to issues such as boundary mismatches, occlusion inconsistencies, and detail drift.

To address these challenges, we propose the Multi-view Geometric Information Extraction Module, which shifts the generation task from the image domain to view-independent proxy surfaces. By establishing a unified geometric representation of the object's shape and topology, we ensure all views share the same geometric structure. As shown in Fig.3, we use GeoWizard [11] to estimate depth and normal maps from the input image, and Rembg [30] to obtain the foreground segmentation mask. The Bilateral Normal Integration (BiNI) algorithm [5] then fuses these inputs into a continuous, edge-preserving surface (BiNI Proxy Surface, BPS). PyVista [41] is then used to render the BPS from the target viewpoint and color it using a normalized normal-based color mapping, producing multi-view geometric images. These images serve as geometric conditional features to guide the multi-view diffusion model's generation process.

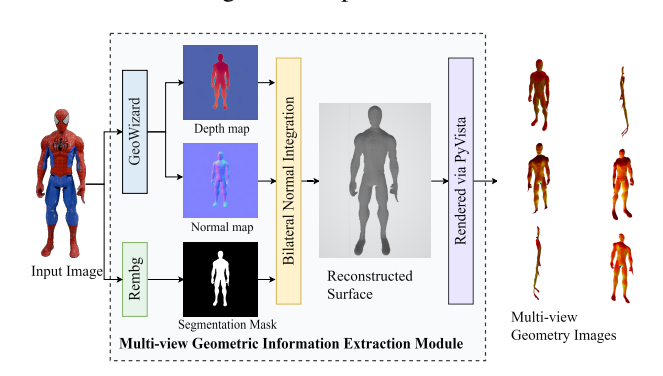


Figure 3. Schematic Diagram of the Multi-view Geometric Information Extraction Module.

This approach ensures that all views are constrained within a unified geometric framework, maintaining the consistency of the object's overall shape, the relative positions of its parts, and the occlusion relationships. Furthermore, normal-based detail cues (such as edges, contours, and subtle curvature variations) provide persistent high-frequency information for the denoising process, effectively reducing detail drift and hallucinated textures. Ultimately, our method ensures cross-view consistency while preserving rich and stable details.

3.2. Conditional Feature Extraction Process

Generating high-quality multi-view results from a single image requires satisfying three key constraints: semantic consistency (consistent object, attributes, and style across views), geometric consistency (coherent shape, structure, and occlusion relationships across views), and appearance fidelity (color and texture consistent with the input image). To meet these constraints, we propose a tri-conditional collaborative constraint method that jointly utilizes cross-modal, geometric, and image information, ensuring both consistency and detail preservation at each denoising step.

As illustrated in Fig.2, our method extracts three types of conditional features:

- Cross-modal Conditional Features: The text prompt and the input image are separately input into the text encoder and image encoder of CLIP, generating two embedding vectors. These vectors are then linearly fused to form the cross-modal feature. This feature is input into the crossattention layer of the U-Net, ensuring consistency in semantic categories, attributes, and style across different views.
- Image Conditional Features: The input image is encoded into a latent representation using a VAE. Noise is added to this latent representation based on the noise level of the current iffusion step. The noisy latent representation is then passed into the U-Net, and input representations are extracted from all self-attention layers to form the image conditional features. The role of the image conditional features is to provide the shape, detail, and texture information of the object, helping the model recover the true appearance of the object and ensuring consistency in structure, shape, and details with the input image.
- Geometric Conditional Features: Multi-view geometric images are encoded into latent representations via a VAE without adding noise. These features are directly input into the U-Net, and input representations are extracted from all self-attention layers to obtain the geometric conditional features. The role of the geometric conditional features is to ensure that the object maintains consistent shape, structure, and occlusion relationships across different views, providing stable geometric constraints and preserving the 3D feel and spatial coherence of the object.

These three types of conditional features are processed through cross-attention and decoupled geometry-enhanced attention layers. The cross-modal conditional features stabilize semantic and style consistency across different views.

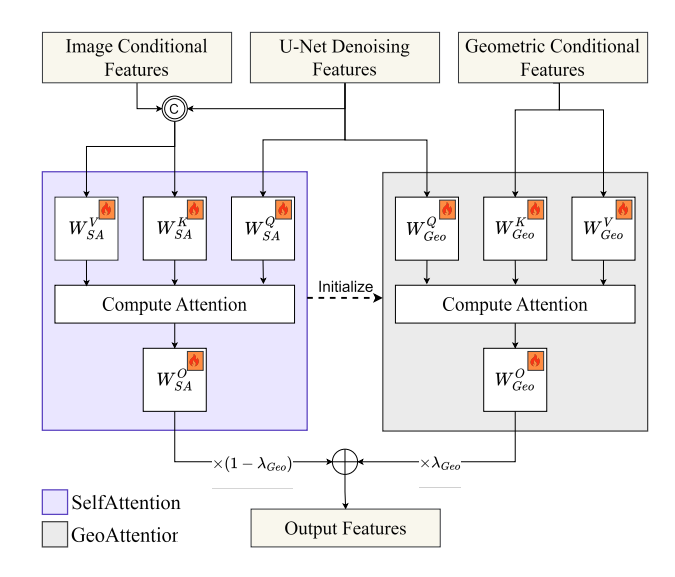


Figure 4. Decoupled Geometry-Enhanced Attention Mechanism

The geometric features provide consistency constraints across views, suppressing perspective distortions and structural mismatches. The image features are responsible for recovering the appearance and mid-to-high frequency details. To ensure that the conditions and the generated target share the same noise scale at each diffusion step, noise is added to the image latent representation, providing matching denoising gradient signals that help stabilize the recovery of color and texture. On the other hand, the geometric features carry high-frequency and strong constraint shape information, and adding noise would weaken their stability and constraint strength across steps. Therefore, they are kept noise-free to consistently apply clear and stable geometric constraints during the denoising process. Through the collaborative effect of these three conditions, the model ensures semantic consistency, structural coherence, and appearance fidelity in the multi-view generation process.

3.3. Decoupled Geometry-Enhanced Attention Mechanism

As shown in the left block diagram of Fig.4, the decoupled geometry-enhanced attention module improves upon the self-attention mechanism of the diffusion model U-Net. This module introduces a parallel attention structure by initializing the geometric attention layers using the same weights as the self-attention layers, allowing parallel processing of both image features and geometric features.

Specifically, the module takes three inputs: image conditional features $F_{\rm img}$, U-Net denoising features $F_{\rm unet}$, and geometric conditional features $F_{\rm Geo}$. In the model, U-Net denoising features $F_{\rm unet}$ serve as the query (Q) input for both attention modules. The image conditional features $F_{\rm img}$ and denoising features $F_{\rm unet}$ are concatenated along the length

dimension to form the key (K) and value (V) inputs for the self-attention layer, while geometric conditional features F_{Geo} are used as the key (K) and value (V) inputs for the geometric attention layer.

In this structure, the two attention modules independently compute attention scores for image and geometric features. The final feature output \mathcal{O} is then obtained by weighted fusion, ensuring consistency and detail recovery for the generated image across multiple views.

The detailed computation process is as follows:

Self-Attention Module (Self Attention): The image conditional features F_{img} and U-Net denoising features F_{unet} are concatenated and linearly transformed using W_{SA} to compute the query (Q), key (K), and value (V). The attention output is then calculated through the self-attention mechanism:

$$Q_{\rm SA} = F_{\rm unet} W_{\rm SA}^Q, \tag{1}$$

$$K_{SA} = (F_{img} \oplus F_{unet})W_{SA}^K, \tag{2}$$

$$V_{\rm SA} = (F_{\rm img} \oplus F_{\rm unet}) W_{\rm SA}^V, \tag{3}$$

$$A_{\rm SA} = \operatorname{Softmax}\left(\frac{Q_{\rm SA}K_{\rm SA}^T}{\sqrt{d_k}}\right)V_{\rm SA} \tag{4}$$

2. Geometric Attention Module (Geo Attention): For the geometric conditional features, the query (Q) is computed using U-Net denoising features $F_{\rm unet}$, while the key (K) and value (V) are derived from the geometric conditional features $F_{\rm Geo}$. The corresponding linear transformations use the geometric attention module's weight matrix $W_{\rm GA}$:

$$Q_{\rm GA} = F_{\rm unet} W_{\rm SA}^Q, \tag{5}$$

$$K_{\rm GA} = F_{\rm Geo} W_{\rm GA}^K, \tag{6}$$

$$V_{\rm GA} = F_{\rm Geo} W_{\rm GA}^V, \tag{7}$$

$$A_{\rm GA} = {\rm Softmax} \left(\frac{Q_{\rm GA} K_{\rm GA}^T}{\sqrt{d_k}} \right) V_{\rm GA} \tag{8}$$

3. Weighted Fusion of Outputs: Finally, the attention outputs of the image conditional and geometric conditional features are fused by weighted summation to produce the final feature output O. The weight coefficient $\lambda_{\rm geo}$ is used to balance the contributions of both features:

$$O = (1 - \lambda_{\text{geo}}) \cdot A_{\text{SA}} W_{\text{SA}}^O + \lambda_{\text{geo}} \cdot A_{\text{GA}} W_{\text{GA}}^O \quad (9)$$

This architecture efficiently processes both image and geometric features simultaneously, ensuring consistency across multiple views and maintaining object shape and detail fidelity. By balancing the weighted fusion, the model avoids over-reliance on either geometric constraints or image details, resulting in more refined and realistic multi-view image generation.

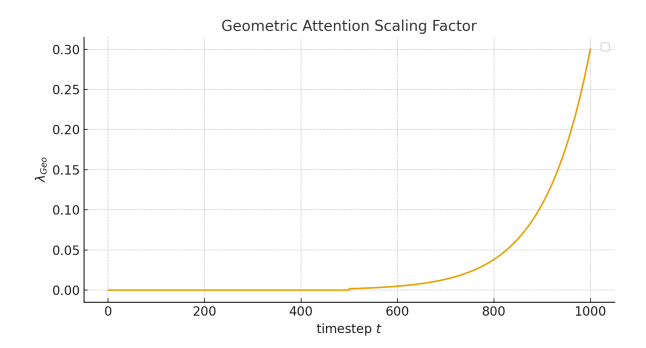


Figure 5. Variation of Geometric Attention Scaling Factor with Diffusion Steps

3.4. Geometric Information Intensity Modulation Mechanism

Based on observations during the experimental process, we applied two adjustments to the geometric conditional features: the Multi-view Geometric Feature Mask and Dynamic Geometric Attention Strength Scheduling.

Multi-view Geometric Feature Mask: Since geometric information is entirely computed from a single image, some views may contain erroneous information. To address this issue, we introduce a cosine similarity-based mechanism that dynamically adjusts the intensity of multi-view geometric features based on the difference between the target and input views, using it as a mask for correction. Specifically, the further a view deviates from the main viewpoint, the less accurate the information becomes, requiring the adjustment of the strength for each view. The adjustment is given by:

$$\tilde{f}_{\text{Geo}}^n = \cos(\Delta\theta_n) \cdot f_{\text{Geo}}^n \tag{10}$$

where f_{Geo}^n represents the geometric feature for the n-th view, and $\Delta \theta_n$ is the deviation between the n-th view and the main viewpoint. The cosine of the angle, $\cos(\Delta \theta_n)$, is used to scale the feature intensity, resulting in the adjusted geometric feature $\tilde{f}_{\mathrm{Geo}}^n$.

Through this adjustment mechanism, we can dynamically scale the geometric feature intensity based on the deviation of each view from the main viewpoint, effectively avoiding the interference of erroneous information and ensuring the consistency and accuracy of the generated geometric features across different views.

Dynamic Geometric Attention Strength Scheduling:

During the experimental process, we observed that in the early stages of the denoising loop, a larger geometric attention scaling factor $\lambda_{\rm geo}$ effectively guides the early denoising process due to the high noise in the generated image. However, as the denoising progresses, the geometric branch may

interfere with the generated result due to modality differences. Therefore, the geometric attention scaling factor $\lambda_{\rm geo}$ should gradually decrease with the timestep. The decay process is shown in Fig.5, where the factor decays from 0.3 to 10^{-5} following a geometric series (i.e., geometric progression), and the scaling factor is set to 0 for the first 500 steps.

$$\lambda_{\text{geo}}(t) = \begin{cases} 0, & \text{if } t \in [0, T//2) \\ 1e^{-5} \cdot \left(\frac{0.3}{1e^{-5}}\right)^{\frac{t-T//2}{T/2}}, & \text{if } t \in [T//2, T] \end{cases}$$

where T is the total number of denoising steps, and t is the current denoising step.

Through these two adjustments, this study effectively controls the influence of geometric information, thereby improving the quality of multi-view generated images. These improvements ensure that at each stage of the generation process, geometric information can precisely guide the denoising process without excessively affecting the details of the final generated image.

4. Experiment

Dataset We trained GeoMVD on a subset of the Objaverse[6] dataset. To construct the training images, we rendered one single-view input image and six ground-truth images using the Cycles[3] engine in Blender. The azimuth and elevation angles of the single-view input image were set to 10° , while the ground-truth images were rendered with azimuth angles evenly distributed from 30° to 330° , with a fixed elevation angle of 0° . All rendered images had a resolution of 320×320 and were in PNG format with an alpha channel.

To evaluate the performance of GeoMVD, we conducted experiments on the Google Scanned Object[9] (GSO) dataset, which is a widely recognized benchmark in the 3D generation field. This dataset is commonly used for performance comparison and validation of related algorithms. Additionally, we tested our method on out-of-domain images collected from the internet to demonstrate its generalization ability. Similarly to previous methods, we removed the background from these out-of-domain images using Rembg and centered the objects.

Implementation Details Our implementation is based on the open-source multi-view diffusion model Zero123++[37], with optimizations built upon this foundation. During training, we integrated LoRA[16] into the self-attention and geometric attention layers of the U-Net, rather than training the entire U-Net, which significantly reduced the number of trainable parameters. The final model had approximately 2.8M trainable parameters. This strategy effectively improved both training efficiency and model performance. We

trained GeoMVD on four GeForce RTX 3090 GPUs with a batch size of 8 and performed 10,000 steps of training. The AdamW optimizer was used, along with a cosine annealing learning rate scheduler. The learning rate started at 5×10^{-5} and gradually decayed to 1.25×10^{-5} , with restarts every 1,000 steps. The entire training process took approximately 15 hours.

4.1. Experimental Results

We compare GeoMVD with Era3D, Zero123++, and MV-Adapter (based on SDXL) in generating multi-view images. All methods generate images from six fixed viewpoints, but the viewpoints differ across the methods. Specifically, GeoMVD, Zero123++, and MV-Adapter use horizontal angles of $\{30^{\circ}, 90^{\circ}, 150^{\circ}, 210^{\circ}, 270^{\circ}, 330^{\circ}\}$, while Era3D generates images from horizontal angles of $\{0^{\circ}, 45^{\circ}, 90^{\circ}, 180^{\circ}, 270^{\circ}, 315^{\circ}\}$. The elevation angles for GeoMVD, Era3D, and MV-Adapter are all 0° , while Zero123++ generates images with varying elevation angles of $\{30^{\circ}, -20^{\circ}, 30^{\circ}, -20^{\circ}, 30^{\circ}, -20^{\circ}\}$. Furthermore, GeoMVD and Era3D use white backgrounds, while Zero123++ and MV-Adapter utilize gray backgrounds.

4.1.1. Qualitative Comparison

Fig.6 presents the generated results of GeoMVD, Era3D, Zero123++, and MV-Adapter on the GSO dataset. The comparison clearly shows that GeoMVD outperforms the other methods in generating consistent multi-view images from a single input. For instance, when generating images of the toaster, gift box, and Mario models, our algorithm produces clear and consistent multi-view images, maintaining superior detail and consistency compared to Era3D and Zero123++, which exhibit artifacts or detail loss in some views. MV-Adapter (based on SDXL) generates blurry images in certain views, lacking a clear structure. Our algorithm successfully preserves morphological consistency across different views and accurately captures details, such as the red stripes on the gift box and the clothing details of Mario, demonstrating its superior performance.

In Fig.7, we show the results of GeoMVD and other methods on out-of-domain images collected from the internet. The comparison highlights the significant advantage of our algorithm in multi-view image generation tasks. Our method maintains consistency across views, generating clear, detail-rich images, while Era3D and Zero123++ show distortions and blurring in certain views, particularly the back and side views of objects. MV-Adapter (SDXL) also suffers from blurriness in detail presentation and fails to effectively represent complex structures, especially in the generation of graphics cards and arcade machines. In contrast, our method accurately restores the geometric shape and details of objects, displaying higher clarity and consistency. Additionally, our approach preserves continuity in shape and detail

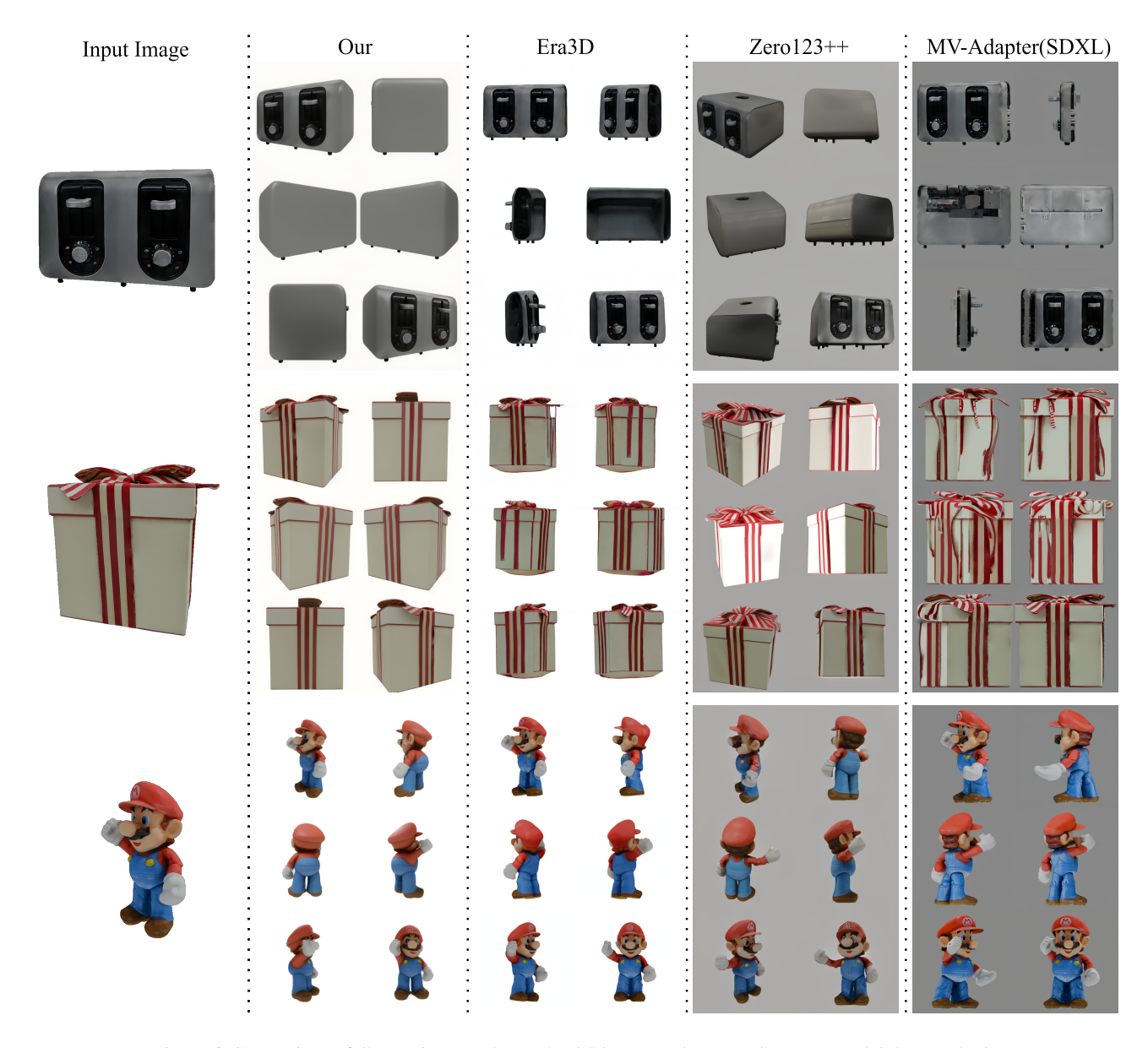


Figure 6. Comparison of Generation Results on the GSO Dataset between GeoMVD and Other Methods.

across multiple views, whereas other methods exhibit unnatural deformations and distortions, especially with complex objects such as toy machines and graphics cards. Overall, our method shows clear advantages in texture, shape, and viewpoint consistency, producing higher-quality multi-view images.

4.1.2. Quantitative Comparison

We evaluated different models on the validation set (a subset of the GSO dataset) using the LPIPS[44], FID[13], and IS[36] metrics. To ensure a fair comparison between the methods, we separately rendered the corresponding ground-truth images for each method and adjusted the background

Table 1. Quantitative Comparison of Image-to-Multi-view Generation on the GSO Dataset between GeoMVD and Other Methods

Model	LPIPS ↓	FID↓	IS ↑
GeoMVD (our)	0.1709	59.0424	13.1779
Era3D	0.2261	63.3328	14.1319
MV-Adapter (SD2)	0.3520	85.4668	15.0358
MV-Adapter (SDXL)	0.3452	77.6760	14.3498
Zero123++	0.2581	63.7488	13.7243

color accordingly, due to variations in background color and viewpoints across the generated images from different mod-

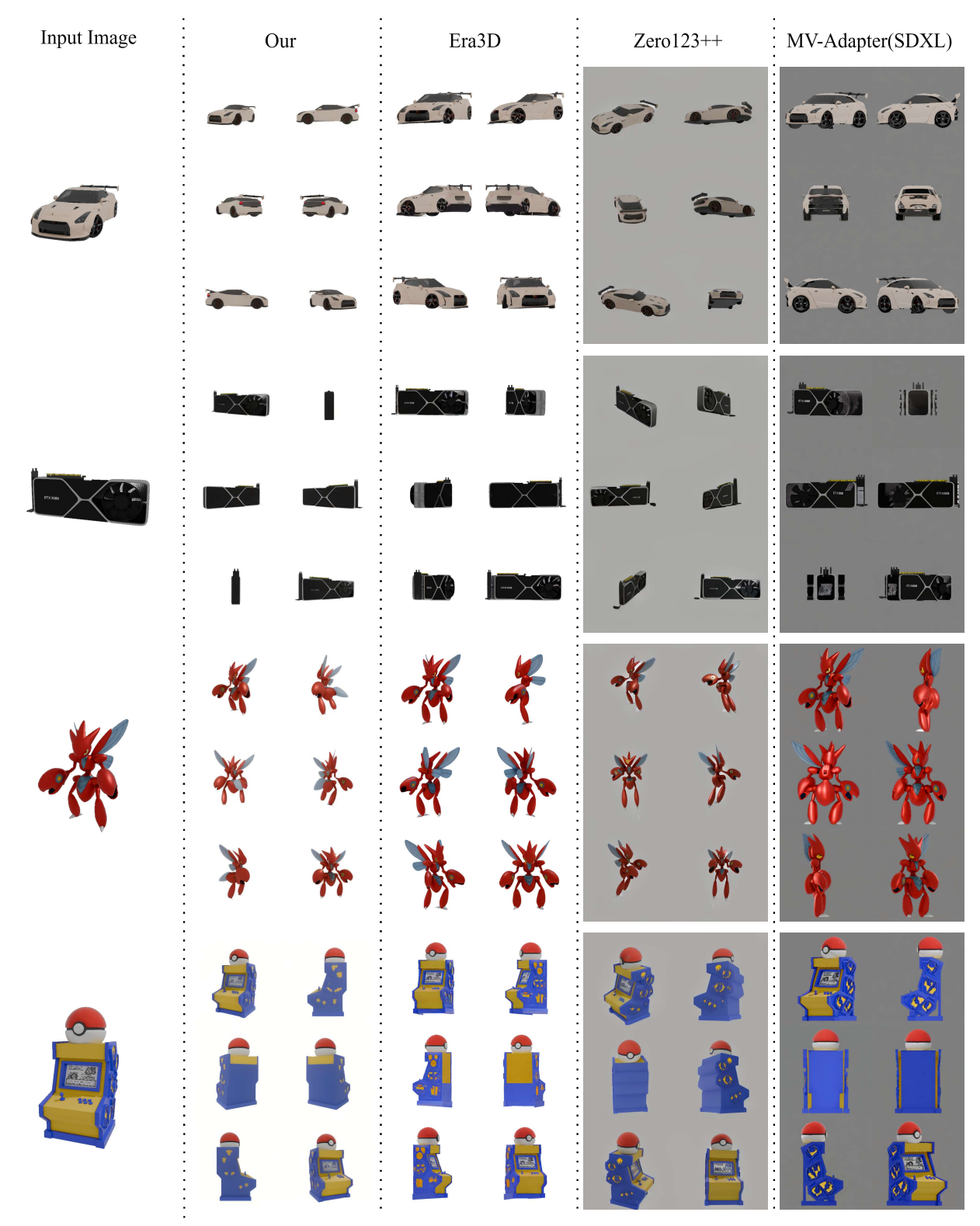


Figure 7. Comparison of Generation Results on Out-of-domain Images from the Internet between GeoMVD and Other Methods.

els. The results are summarized in Table 1. Experimental results show that our GeoMVD demonstrates a clear advantage in both generation quality and viewpoint consistency, producing higher-quality multi-view images.

4.2. Ablation Experiment

To validate the effectiveness of the proposed architecture, we conducted a series of ablation experiments to analyze the impact of each key component on the final results. By progressively removing the three input features and related components upon which the model depends, we can evaluate the contribution of each module to the model's overall performance. The experimental design is outlined as follows:

Removal of Cross-modal Conditional Features: To assess the impact of cross-modal features, we set the input CLIP image to a blank image and the text prompt to an empty string. This experiment aims to evaluate how the absence of cross-modal features affects the consistency and detail preservation in the generated outputs.

Removal of Image Conditional Features: In this experiment, we remove the image conditional features, meaning the image no longer contributes to the decoupled geometry-enhanced attention calculation. The goal is to assess the role of image conditional features in the appearance and detail of the generated image, as well as their impact on the denoising process.

Multi-view Geometric Conditional Features: We also conducted a series of ablation experiments on multi-view geometric conditional features, which are divided into the following scenarios:

- Removal of Geometric Attention Branch: In this experiment, we completely remove the geometric attention branch, meaning that geometric attention is no longer utilized during the denoising process. The purpose of this experiment is to verify whether the geometric attention branch is crucial for the quality and consistency of the generated images.
- 2. Removal of Geometric Feature Mask: In this experiment, we remove the cosine similarity-based dynamic intensity adjustment mechanism, meaning that the intensity of geometric features is no longer adjusted based on the deviation between the target and input views. As a result, the geometric feature intensity for all views remains constant, regardless of their deviation from the main viewpoint. This experiment aims to evaluate the impact of missing geometric feature intensity modulation on the geometric consistency and accuracy of the generated images, as well as the interference of erroneous information on the final results.

3. Removal of Dynamic Geometric Attention Strength Scheduling: In this experiment, we fix the geometric attention scaling factor $\lambda_{\rm geo}$, meaning that the strength of this factor is no longer dynamically adjusted based on the time step during the denoising process. Unlike the normal dynamic decay process, the geometric attention scaling factor will remain constant in this experiment. The purpose of this experiment is to assess the impact of the absence of dynamic decay in the geometric attention scaling factor on the final results, particularly whether a high fixed geometric attention factor interferes with image details and negatively affects the quality and consistency of the generated image.

4.2.1. Quantitative Comparison of Ablation Experiments

Table2 presents the quantitative comparison results of different ablation experiments. The experimental results clearly show that geometric attention, geometric feature masks, and dynamic geometric attention strength scheduling play crucial roles in the quality of the generated images. Removing these modules leads to significant degradation in consistency, detail, and diversity of the generated images. In particular, the interaction between image conditional features and geometric conditional features, the modulation of geometric feature intensity, and the dynamic adjustment of the attention mechanism are all essential for the denoising process. These experiments validate the effectiveness of the proposed architecture and provide a basis for further optimization. Qualitative Comparison of Ablation Experiments can be found in the appendix A.

Table 2. Quantitative Comparison in Ablation Experiments

Ablation Methods	LPIPS ↓	FID↓	IS ↑
GeoMVD (Our)	0.1709	59.0424	13.1779
w/o Cross-modal Condi-	0.1934	67.8664	13.9451
tional Features			
w/o Image Conditional	0.3075	131.8195	9.1374
Features			
w/o Geometric Attention	0.1795	61.5617	12.7903
Branch			
w/o Geometric Feature	0.1760	61.1665	12.8486
Mask	0.2624	02.0276	12 2201
w/o Dynamic Geomet-	0.2624	83.8276	13.2391
ric Attention Strength Scheduling			
Scheduling			

4.2.2. Analysis and Discussion

The following is an analysis and discussion of the results from each experimental setup:

Removal of Cross-modal Conditional Features: Cross-modal conditional features, which combine image and text,

provide essential cross-modal guidance within the model. After removing these features, the consistency of the generated images across different views significantly deteriorates, resulting in distortions and unnatural effects. This emphasizes the critical role of cross-modal features in maintaining the consistency of generated images. The combination of image and text not only provides richer semantic information but also reduces distortions during multi-view generation, ensuring the consistency of the object's shape. Thus, cross-modal features are indispensable for the naturalness and consistency of generated images across different views.

Removal of Image Conditional Features: When the image conditional features are removed, the model is unable to accurately understand or restore the object's shape and details, leading to a complete degradation of the generated outputs. The object loses its original structure, shape, detail, and consistency. This result underscores the crucial role of image conditional features in preserving the appearance, detail, and geometric consistency of the object. Without image guidance, the overall quality of the generated image is significantly reduced, leading to a loss of realism and detail. This highlights the importance of image conditional features for the quality of the generated results.

Geometric Features and Condition Analysis: The role of geometric features in multi-view generation models is crucial and manifests in several key aspects:

- Shape Consistency: Geometric features ensure that the object maintains consistent shape and structure across different views, preventing distortions or inconsistencies in shape between views.
- **Structural Coherence:** Geometric features help maintain correct occlusion relationships and relative positioning across views, ensuring that the object appears natural from all perspectives.
- Detail Restoration: During the denoising process, geometric features provide high-frequency information such as edges and contours, aiding in the restoration of object details and enhancing clarity and precision in the generated image.

The effectiveness of geometric conditions depends on their strength. When the geometric condition is too weak, overly strong, or improperly controlled, it significantly impacts the generation quality of multi-view images. Specifically:

Weak Geometric Condition Strength (Removal of Geometric Attention Branch): When the geometric condition is too weak, the consistency of shape and structure across different views deteriorates significantly. After removing the geometric attention branch, the object's structure and shape fail to remain consistent across multiple

- views, especially in the generation of complex objects, where the shape appears blurry and fragmented. The lack of necessary geometric constraints leads to a loss of structure and spatial coherence in the generated images.
- 2. Improper Geometric Condition Strength Control (Removal of Geometric Feature Mask): The geometric feature mask adjusts the intensity of geometric information across different views, ensuring shape consistency. After removing the geometric feature mask, the geometric structure of the object fails to align correctly across different views, particularly in the generation of complex objects. Occlusion relationships and shape deviations emerge, causing geometric inconsistencies in the generated images. Without the geometric feature mask, the object's structure becomes incoherent, which negatively affects image quality.
- 3. Excessive Geometric Condition Strength (Removal of Dynamic Geometric Attention Strength Scheduling):

 The geometric feature mask adjusts the intensity of geometric information across different views, ensuring shape consistency. After removing the geometric feature mask, the geometric structure of the object fails to align correctly across views, especially for complex objects. Occlusion relationships and shape deviations emerge, causing geometric inconsistencies in the generated images. Without the geometric feature mask, the object's structure becomes incoherent, which negatively impacts image quality.

In conclusion, geometric conditions play a crucial role in generating multi-view images by ensuring shape consistency, structural coherence, and detail restoration. When geometric conditions are too strong, the generated images suffer from excessive constraints, leading to distortions and unnatural details. When geometric conditions are too weak, the lack of consistency in object shape causes the images to lose coherence and realism across views. Improper control of geometric information results in geometric inconsistencies, where the generated images fail to align across views. Proper adjustment of geometric condition strength is key to generating high-quality images. By applying appropriate geometric constraints, the model ensures shape consistency while restoring details and maintaining the naturalness and accuracy of the images.

5. Conclusion

This paper proposes a Geometry-guided Multi-view Diffusion Model (GeoMVD) designed to address the challenge of generating consistent multi-view images from a single input image. We introduce several key components, including a multi-view geometric detail extraction module, a conditional feature extraction process, a decoupled geometry-enhanced attention mechanism, and a geometric information inten-

sity modulation mechanism. These components significantly enhance the quality, consistency, and detail fidelity of the generated images. Experimental results on multiple datasets demonstrate that GeoMVD outperforms existing methods, particularly in terms of detail preservation and cross-view consistency.

However, there are still some limitations in this study. First, while the multi-view geometric detail extraction module effectively resolves the issue of geometric consistency, the process remains relatively complex and computationally expensive. Second, the model's adjustment of geometric features may not be sufficiently fine-tuned for complex scenes, limiting the naturalness and detailed representation of the generated images.

Future work will focus on several areas: (1) improving the efficiency and accuracy of geometric information extraction to reduce computational costs, (2) enhancing the model's ability to generalize and adapt to a broader range of scenes and object types, and (3) expanding the integration of multimodal information to mprove the model's cross-domain applicability. Through these efforts, we aim to further advance the practical application of multi-view generation models, especially in fields such as virtual reality, augmented reality, and autonomous driving.

References

- [1] Stephen Batifol, Andreas Blattmann, Frederic Boesel, Saksham Consul, Cyril Diagne, Tim Dockhorn, Jack English, Zion English, Patrick Esser, Sumith Kulal, et al. Flux. 1 kontext: Flow matching for in-context image generation and editing in latent space. *arXiv e-prints*, pages arXiv–2506, 2025. 1, 3
- [2] James Betker, Gabriel Goh, Li Jing, Tim Brooks, Jianfeng Wang, Linjie Li, Long Ouyang, Juntang Zhuang, Joyce Lee, Yufei Guo, et al. Improving image generation with better captions. *Computer Science. https://cdn. openai.com/papers/dall-e-3. pdf*, 2(3):8, 2023. 1
- [3] Blender Foundation. Cycles rendering engine blender features. https://www.blender.org/features/rendering/#cycles, 2025. Accessed: 2025-11-07. 7
- [4] Siyu Cao, Hangting Chen, Peng Chen, Yiji Cheng, Yutao Cui, Xinchi Deng, Ying Dong, Kipper Gong, Tianpeng Gu, Xiusen Gu, et al. Hunyuanimage 3.0 technical report. *arXiv preprint arXiv:2509.23951*, 2025. 3
- [5] Xu Cao, Hiroaki Santo, Boxin Shi, Fumio Okura, and Yasuyuki Matsushita. Bilateral normal integration. In *European Conference on Computer Vision*, pages 552–567. Springer, 2022. 4
- [6] Matt Deitke, Dustin Schwenk, Jordi Salvador, Luca Weihs, Oscar Michel, Eli VanderBilt, Ludwig Schmidt, Kiana Ehsani, Aniruddha Kembhavi, and Ali Farhadi. Objaverse: A universe of annotated 3d objects. In *Proceedings of the IEEE/CVF* conference on computer vision and pattern recognition, pages 13142–13153, 2023. 3, 7

- [7] Zijun Deng, Xiangteng He, Yuxin Peng, Xiongwei Zhu, and Lele Cheng. Mv-diffusion: Motion-aware video diffusion model. In *Proceedings of the 31st ACM International Conference on Multimedia*, pages 7255–7263, 2023. 1, 3
- [8] Prafulla Dhariwal and Alexander Nichol. Diffusion models beat gans on image synthesis. Advances in neural information processing systems, 34:8780–8794, 2021. 3
- [9] Laura Downs, Anthony Francis, Nate Koenig, Brandon Kinman, Ryan Hickman, Krista Reymann, Thomas B McHugh, and Vincent Vanhoucke. Google scanned objects: A high-quality dataset of 3d scanned household items. In 2022 International Conference on Robotics and Automation (ICRA), pages 2553–2560. IEEE, 2022. 7
- [10] Patrick Esser, Sumith Kulal, Andreas Blattmann, Rahim Entezari, Jonas Müller, Harry Saini, Yam Levi, Dominik Lorenz, Axel Sauer, Frederic Boesel, et al. Scaling rectified flow transformers for high-resolution image synthesis. In *Forty-first international conference on machine learning*, 2024. 1, 3
- [11] Xiao Fu, Wei Yin, Mu Hu, Kaixuan Wang, Yuexin Ma, Ping Tan, Shaojie Shen, Dahua Lin, and Xiaoxiao Long. Geowizard: Unleashing the diffusion priors for 3d geometry estimation from a single image. In *European Conference on Computer Vision*, pages 241–258. Springer, 2024. 4
- [12] Ruiqi Gao, Aleksander Holynski, Philipp Henzler, Arthur Brussee, Ricardo Martin-Brualla, Pratul Srinivasan, Jonathan T Barron, and Ben Poole. Cat3d: Create anything in 3d with multi-view diffusion models. *arXiv preprint arXiv:2405.10314*, 2024. 1, 3
- [13] Martin Heusel, Hubert Ramsauer, Thomas Unterthiner, Bernhard Nessler, and Sepp Hochreiter. Gans trained by a two time-scale update rule converge to a local nash equilibrium. Advances in neural information processing systems, 30, 2017.
- [14] Jonathan Ho and Tim Salimans. Classifier-free diffusion guidance. *arXiv preprint arXiv:2207.12598*, 2022. 3
- [15] Jonathan Ho, Ajay Jain, and Pieter Abbeel. Denoising diffusion probabilistic models. *Advances in neural information processing systems*, 33:6840–6851, 2020. 3
- [16] Edward J Hu, Yelong Shen, Phillip Wallis, Zeyuan Allen-Zhu, Yuanzhi Li, Shean Wang, Lu Wang, Weizhu Chen, et al. Lora: Low-rank adaptation of large language models. *ICLR*, 1(2):3, 2022. 7
- [17] Zehuan Huang, Hao Wen, Junting Dong, Yaohui Wang, Yang-guang Li, Xinyuan Chen, Yan-Pei Cao, Ding Liang, Yu Qiao, Bo Dai, et al. Epidiff: Enhancing multi-view synthesis via localized epipolar-constrained diffusion. In *Proceedings of the IEEE/CVF Conference on Computer Vision and Pattern Recognition*, pages 9784–9794, 2024. 1, 3
- [18] Zehuan Huang, Yuan-Chen Guo, Haoran Wang, Ran Yi, Lizhuang Ma, Yan-Pei Cao, and Lu Sheng. Mv-adapter: Multi-view consistent image generation made easy. In *Proceedings of the IEEE/CVF International Conference on Computer Vision*, pages 16377–16387, 2025. 3
- [19] Yoonwoo Jeong, Jinwoo Lee, Chiheon Kim, Minsu Cho, and Doyup Lee. Nvs-adapter: Plug-and-play novel view synthesis from a single image. In *European Conference on Computer Vision*, pages 449–466. Springer, 2024. 3

- [20] Yash Kant, Aliaksandr Siarohin, Ziyi Wu, Michael Vasilkovsky, Guocheng Qian, Jian Ren, Riza Alp Guler, Bernard Ghanem, Sergey Tulyakov, and Igor Gilitschenski. Spad: Spatially aware multi-view diffusers. In *Proceedings of the IEEE/CVF Conference on Computer Vision and Pattern Recognition*, pages 10026–10038, 2024. 1, 3
- [21] Peng Li, Yuan Liu, Xiaoxiao Long, Feihu Zhang, Cheng Lin, Mengfei Li, Xingqun Qi, Shanghang Zhang, Wei Xue, Wenhan Luo, et al. Era3d: High-resolution multiview diffusion using efficient row-wise attention. Advances in Neural Information Processing Systems, 37:55975–56000, 2024. 1, 3
- [22] Chendi Lin, Heshan Liu, Qunshu Lin, Zachary Bright, Shitao Tang, Yihui He, Minghao Liu, Ling Zhu, and Cindy Le. Objaverse++: Curated 3d object dataset with quality annotations. arXiv preprint arXiv:2504.07334, 2025. 3
- [23] Yaron Lipman, Ricky TQ Chen, Heli Ben-Hamu, Maximilian Nickel, and Matt Le. Flow matching for generative modeling. arXiv preprint arXiv:2210.02747, 2022. 3
- [24] Ruoshi Liu, Rundi Wu, Basile Van Hoorick, Pavel Tokmakov, Sergey Zakharov, and Carl Vondrick. Zero-1-to-3: Zero-shot one image to 3d object. In *Proceedings of the IEEE/CVF* international conference on computer vision, pages 9298– 9309, 2023. 3
- [25] Yuan Liu, Cheng Lin, Zijiao Zeng, Xiaoxiao Long, Lingjie Liu, Taku Komura, and Wenping Wang. Syncdreamer: Generating multiview-consistent images from a single-view image. arXiv preprint arXiv:2309.03453, 2023. 1, 3
- [26] Xiaoxiao Long, Yuan-Chen Guo, Cheng Lin, Yuan Liu, Zhiyang Dou, Lingjie Liu, Yuexin Ma, Song-Hai Zhang, Marc Habermann, Christian Theobalt, et al. Wonder3d: Single image to 3d using cross-domain diffusion. In *Proceedings of the IEEE/CVF conference on computer vision and pattern recognition*, pages 9970–9980, 2024. 1, 3
- [27] Alex Nichol, Prafulla Dhariwal, Aditya Ramesh, Pranav Shyam, Pamela Mishkin, Bob McGrew, Ilya Sutskever, and Mark Chen. Glide: Towards photorealistic image generation and editing with text-guided diffusion models. arXiv preprint arXiv:2112.10741, 2021. 1
- [28] William Peebles and Saining Xie. Scalable diffusion models with transformers. In *Proceedings of the IEEE/CVF inter*national conference on computer vision, pages 4195–4205, 2023. 3
- [29] Dustin Podell, Zion English, Kyle Lacey, Andreas Blattmann, Tim Dockhorn, Jonas Müller, Joe Penna, and Robin Rombach. Sdxl: Improving latent diffusion models for high-resolution image synthesis. arXiv preprint arXiv:2307.01952, 2023. 1, 3
- [30] Xuebin Qin, Zichen Zhang, Chenyang Huang, Masood Dehghan, Osmar R Zaiane, and Martin Jagersand. U2-net: Going deeper with nested u-structure for salient object detection. Pattern recognition, 106:107404, 2020. 4
- [31] Alec Radford, Jong Wook Kim, Chris Hallacy, Aditya Ramesh, Gabriel Goh, Sandhini Agarwal, Girish Sastry, Amanda Askell, Pamela Mishkin, Jack Clark, et al. Learning transferable visual models from natural language supervision. In *International conference on machine learning*, pages 8748–8763. PmLR, 2021. 3

- [32] Colin Raffel, Noam Shazeer, Adam Roberts, Katherine Lee, Sharan Narang, Michael Matena, Yanqi Zhou, Wei Li, and Peter J Liu. Exploring the limits of transfer learning with a unified text-to-text transformer. *Journal of machine learning* research, 21(140):1–67, 2020. 3
- [33] Aditya Ramesh, Prafulla Dhariwal, Alex Nichol, Casey Chu, and Mark Chen. Hierarchical text-conditional image generation with clip latents. arXiv preprint arXiv:2204.06125, 1(2): 3, 2022. 1, 3
- [34] Robin Rombach, Andreas Blattmann, Dominik Lorenz, Patrick Esser, and Björn Ommer. High-resolution image synthesis with latent diffusion models. In *Proceedings of* the IEEE/CVF conference on computer vision and pattern recognition, pages 10684–10695, 2022. 3
- [35] Chitwan Saharia, William Chan, Saurabh Saxena, Lala Li, Jay Whang, Emily L Denton, Kamyar Ghasemipour, Raphael Gontijo Lopes, Burcu Karagol Ayan, Tim Salimans, et al. Photorealistic text-to-image diffusion models with deep language understanding. Advances in neural information processing systems, 35:36479–36494, 2022. 1
- [36] Tim Salimans, Ian Goodfellow, Wojciech Zaremba, Vicki Cheung, Alec Radford, and Xi Chen. Improved techniques for training gans. Advances in neural information processing systems, 29, 2016. 8
- [37] Ruoxi Shi, Hansheng Chen, Zhuoyang Zhang, Minghua Liu, Chao Xu, Xinyue Wei, Linghao Chen, Chong Zeng, and Hao Su. Zero123++: a single image to consistent multi-view diffusion base model. arXiv preprint arXiv:2310.15110, 2023.
 1, 3, 7
- [38] Yichun Shi, Peng Wang, Jianglong Ye, Mai Long, Kejie Li, and Xiao Yang. Mvdream: Multi-view diffusion for 3d generation. arXiv preprint arXiv:2308.16512, 2023. 1, 3
- [39] Jiaming Song, Chenlin Meng, and Stefano Ermon. Denoising diffusion implicit models. arXiv preprint arXiv:2010.02502, 2020. 3
- [40] Shitao Tang, Jiacheng Chen, Dilin Wang, Chengzhou Tang, Fuyang Zhang, Yuchen Fan, Vikas Chandra, Yasutaka Furukawa, and Rakesh Ranjan. Mvdiffusion++: A dense highresolution multi-view diffusion model for single or sparseview 3d object reconstruction. In European Conference on Computer Vision, pages 175–191. Springer, 2024. 1, 3
- [41] The PyVista Developers. Pyvista: 3d plotting and mesh analysis in python. https://pyvista.org/, 2019. Accessed: 2025-11-07. 4
- [42] Peng Wang and Yichun Shi. Imagedream: Image-prompt multi-view diffusion for 3d generation. arXiv preprint arXiv:2312.02201, 2023. 1
- [43] Xianggang Yu, Mutian Xu, Yidan Zhang, Haolin Liu, Chongjie Ye, Yushuang Wu, Zizheng Yan, Chenming Zhu, Zhangyang Xiong, Tianyou Liang, et al. Mvimgnet: A largescale dataset of multi-view images. In *Proceedings of the IEEE/CVF conference on computer vision and pattern recog*nition, pages 9150–9161, 2023. 3
- [44] Richard Zhang, Phillip Isola, Alexei A Efros, Eli Shechtman, and Oliver Wang. The unreasonable effectiveness of deep features as a perceptual metric. In *Proceedings of the IEEE* conference on computer vision and pattern recognition, pages 586–595, 2018. 8

- [45] Rui Zhang, Yaosen Chen, Yuegen Liu, Wei Wang, Xuming Wen, and Hongxia Wang. Tvg: A training-free transition video generation method with diffusion models. *IEEE Trans*actions on Circuits and Systems for Video Technology, 2025.
- [46] Chuanxia Zheng and Andrea Vedaldi. Free3d: Consistent novel view synthesis without 3d representation. In *Proceedings of the IEEE/CVF Conference on Computer Vision and Pattern Recognition*, pages 9720–9731, 2024. 1, 3

A. Qualitative Comparison of Ablation Experiments

Removal of Cross-modal Conditional Features: After removing the cross-modal conditional features, the quality of the generated multi-view images significantly decreases. As shown in Fig.8, the morphological consistency of the object across different views is compromised, with some views exhibiting shape distortions and improper structural alignment. For instance, the details of the sofa and chair, particularly in terms of texture and fabric representation, are lost, severely affecting the realism of the generated images. Additionally, removing the cross-modal conditional features disrupts the consistency of color and texture, making the generated objects appear visually unnatural. These results highlight the crucial role of cross-modal conditional features in maintaining consistency and detail fidelity in multi-view image generation.

Removal of Image Conditional Features: After removing the image conditional features, the generated multi-view images lose their original consistency and detail restoration capabilities. As shown in Fig.9, in the absence of image conditional features, the generated objects exhibit significant distortion and inconsistency in both shape and texture across multiple views. The details of the objects, such as edges, contours, and surface structure, fail to maintain coherence across different viewpoints, resulting in blurry images that lack realism. The accuracy of the overall shape and the fidelity of details notably decrease, particularly in the reconstruction of complex structures and surface textures. These results demonstrate that image conditional features are essential for ensuring consistency and detail recovery in generated images, and their absence leads to a substantial decline in the quality of the generated results.

Removal of Geometric Attention Branch: As shown in Fig. 10, after removing the geometric attention branch, the quality of the generated multi-view images significantly declines in terms of shape consistency and detail restoration. The geometric structure of the object fails to remain consistent across different views, resulting in distorted shapes and unnatural variations. Occlusion relationships and the relative positions of the objects are also not properly coordinated across views, leading to a lack of spatial coherence in the generated results. Moreover, the performance of finer details is unstable, with a weakened ability to restore object edges, textures, and small structures, resulting in blurred and distorted outputs. The absence of the geometric attention branch weakens the geometric constraints on the image, causing inconsistencies in shape and details across multiple views. Therefore, the geometric attention branch plays a critical role in ensuring the consistency, detail fidelity, and

structural coherence of multi-view images, and its removal significantly impacts the quality and naturalness of the generated results.

Removal of Geometric Feature Mask: After removing the geometric feature mask, the quality of the generated multi-view images significantly deteriorates. As shown in Fig.11, the consistency of the object's shape and details is compromised, particularly in maintaining the geometric structure and occlusion relationships. The shapes of the generated backpack and boots are inaccurate, especially on the back and bottom of the backpack, where the shape becomes distorted. The geometric feature mask ensures consistency in shape and occlusion relationships across different views by adjusting the intensity of the geometric information. Without this mask, the structure and shape of the objects fail to align properly across views, resulting in geometric inconsistencies in the generated outputs. Furthermore, the generated basket and boots lose their structural integrity across multiple views, with severe detail loss, especially in surface and fine details. Without the support of the geometric feature mask, the structure of the objects becomes blurred. Overall, the geometric feature mask provides stable geometric constraints during the generation process, ensuring the 3D feel and spatial coherence of the objects. Its removal leads to a lack of consistency in the shape and structure of the generated images.

Removal of Dynamic Geometric Attention Strength **Scheduling:** As shown in Fig. 12, after removing the dynamic geometric attention strength scheduling, the generated multi-view images exhibit noticeable issues in shape consistency and detail restoration. The geometric structure and surface details of the object fail to remain consistent across different views, resulting in distortions in shape and structure between multiple views. Notably, the handling of surface details and textures in the generated images shows unnatural gloss and blurriness, particularly in the finer details. This indicates that dynamic geometric attention strength scheduling is crucial for ensuring geometric consistency, detail fidelity, and structural coherence across different views. Its absence leads to deviations in object shape and loss of detail, negatively impacting the quality and naturalness of the generated images.

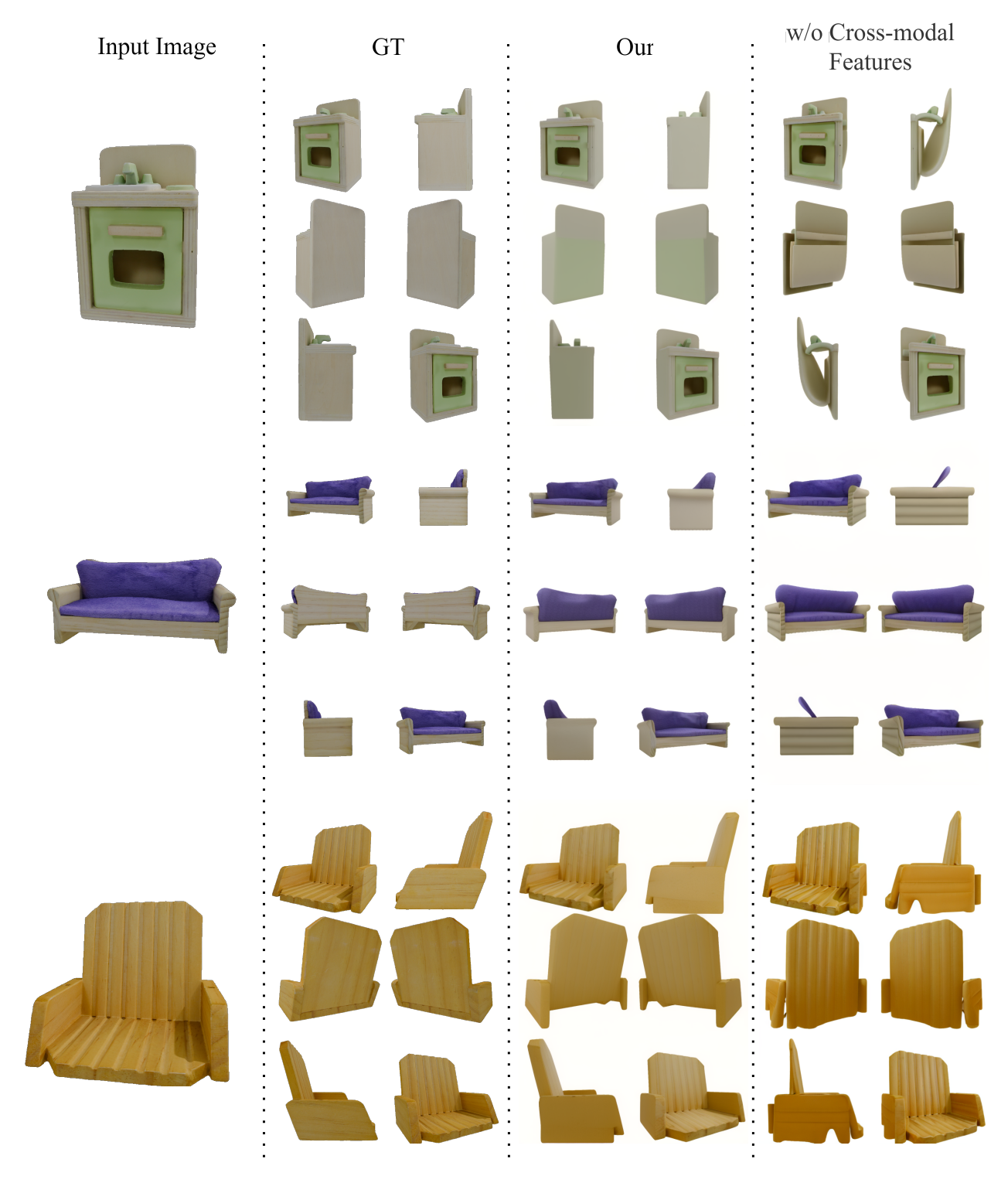


Figure 8. Removal of Cross-modal Conditional Features.

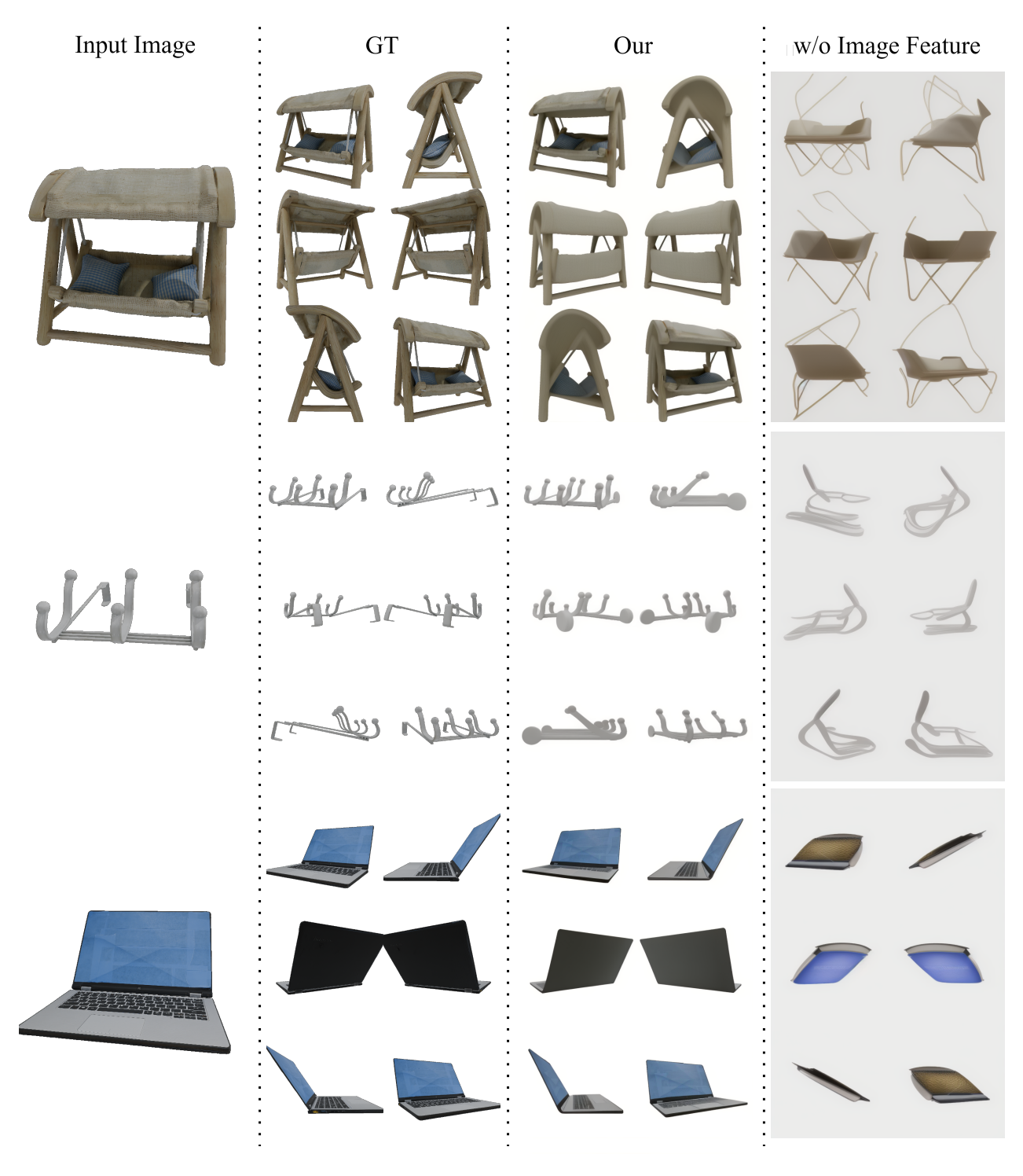


Figure 9. Removal of Image Conditional Features.



Figure 10. Removal of Geometric Attention Branch



Figure 11. Removal of Geometric Feature Mask



Figure 12. Removal of Dynamic Geometric Attention Strength Scheduling